

Universal quantum control based on parametric modulation in superconducting circuits

Dan-Yu Li(李丹宇), Ji Chu(储继), Wen Zheng(郑文), Dong Lan(兰栋), Jie Zhao(赵杰), Shao-Xiong Li(李邵雄), Xin-Sheng Tan(谭新生), and Yang Yu(于扬)

Citation: Chin. Phys. B, 2021, 30 (**7**): 070308. DOI: 10.1088/1674-1056/ac01c3
Journal homepage: http://cpb.iphy.ac.cn; http://iopscience.iop.org/cpb

What follows is a list of articles you may be interested in

Invariants-based shortcuts for fast generating Greenberger—Horne—Zeilinger state among three superconducting qubits

Jing Xu(徐晶), Lin Yu(于琳), Jin-Lei Wu(吴金雷), Xin Ji(计新)
Chin. Phys. B, 2017, 26 (**9**): 090301. DOI: 10.1088/1674-1056/26/9/090301

Fast generating *W* state of three superconducting qubits via Lewis-Riesenfeld invariants

Lin Yu(于琳), Jing Xu(徐晶), Jin-Lei Wu(吴金雷), Xin Ji(计新)
Chin. Phys. B, 2017, 26 (**6**): 060306. DOI: 10.1088/1674-1056/26/6/060306

Creating nitrogen–vacancy ensembles in diamond for coupling with flux qubit

Ya-Rui Zheng(郑亚锐), Jian Xing(邢健), Yan-Chun Chang(常彦春), Zhi-Guang Yan(闫智广), Hui Deng(邓辉), Yu-Lin Wu(吴玉林), Li Lü(吕力), Xin-Yu Pan(潘新宇), Xiao-Bo Zhu(朱晓波), Dong-Ning Zheng(郑东宁)
Chin. Phys. B, 2017, 26 (**2**): 020305. DOI: 10.1088/1674-1056/26/2/020305

Design of a gap tunable flux qubit with FastHenry

Naheed Akhtar, Yarui Zheng(郑亚锐), Mudassar Nazir, Yulin Wu(吴玉林), Hui Deng(邓辉), Dongning Zheng(郑东宁), Xiaobo Zhu(朱晓波)
Chin. Phys. B, 2016, 25 (**12**): 120305. DOI: 10.1088/1674-1056/25/12/120305

Dynamical decoupling pulses on the quantum correlations for the system of superconducting quantum circuit

Wang Dong-Mei, Qian Yi, Xu Jing-Bo, Yu You-Hong
Chin. Phys. B, 2015, 24 (**11**): 110304. DOI: 10.1088/1674-1056/24/11/110304

SPECIAL TOPIC — Quantum computation and quantum simulation

Universal quantum control based on parametric modulation in superconducting circuits*

Dan-Yu Li(李丹宇)[1], Ji Chu(储继)[2], Wen Zheng(郑文)[1], Dong Lan(兰栋)[1], Jie Zhao(赵杰)[1], Shao-Xiong Li(李邵雄)[1,†], Xin-Sheng Tan(谭新生)[1,‡], and Yang Yu(于扬)[1]

[1] *National Laboratory of Solid State Microstructures, School of Physics, Nanjing University, Nanjing* 210093, *China*
[2] *Shenzhen Institute for Quantum Science and Engineering, Southern University of Science and Technology, Shenzhen* 518055, *China*

(Received 25 February 2021; revised manuscript received 30 April 2021; accepted manuscript online 16 May 2021)

As superconducting quantum circuits are scaling up rapidly towards the noisy intermediate-scale quantum (NISQ) era, the demand for electronic control equipment has increased significantly. To fully control a quantum chip of N qubits, the common method based on up-conversion technology costs at least $2 \times N$ digital-to-analog converters (DACs) and N IQ mixers. The expenses and complicate mixer calibration have become a hinderance for intermediate-scale quantum control. Here we propose a universal control scheme for superconducting circuits, fully based on parametric modulation. To control N qubits on a chip, our scheme only requires N DACs and no IQ mixer, which significantly reduces the expenses. One key idea in the control scheme is to introduce a global pump signal for single-qubit gates. We theoretically explain how the universal gates are constructed using parametric modulation. The fidelity analysis shows that parametric single-qubit (two-qubit) gates in the proposed scheme can achieve low error rates of 10^{-4}, with a gate time of about 60 ns (100 ns).

Keywords: superconducting qubits, parametric modulation, single-qubit gate, iSWAP gate

PACS: 03.67.Lx **DOI:** 10.1088/1674-1056/ac01c3

1. Introduction

Recent progress shows that superconducting quantum circuit is one of the most promising candidates for quantum computing.[1–4] While quantum chips with hundreds of qubits can be expected in the near future,[5,6] the expansion of electronic devices for quantum control has become a significant problem. There is an urgent need for a scalable and economical control scheme.

The frequency of superconducting qubits generally lies in a range of 4 GHz–10 GHz.[7–9] To manipulate the qubits, sequences of microwave pulses with a duration from tens to hundreds of nanoseconds are injected into the quantum chip through control lines. Although such microwave pulses can be directly generated by digital-to-analog converters (DACs) with a high sampling rate,[10,11] the instruments are not economical for widespread integration. Currently, the up-conversion technology is widely used. The microwave signal is produced by mixing up a continuous microwave with intermediate frequency (IF) pulses, utilizing an IQ mixer. The IF pulses are produced by DACs with sampling rates of a few gigahertz. This method has the following drawbacks: (i) Each qubit requires at least two DACs and an IQ mixer for up-conversion, which has become a great cost when scaling up; (ii) Since the electrical performance of the mixer varies due to manufacturing and environmental influence, regular calibration is necessary to suppress image tones and carrier leakage.[12] The careful calibration of hundreds of IQ mixers regularly becomes a daunting task in real experiments. Besides, additional hardware is needed for the calibration, such as spectrum analyzers. To alleviate these problems, some efforts have been made recently by hardware improvement.[13,14]

In this paper, we propose a simple and economical universal control scheme based on parametric modulation,[15–20] which provides a solution from another aspect. In the scheme, a continuous microwave signal is used as a global pump for all qubits in the chip. Each qubit is individually controlled by a sub-GHz parametric signal through its Z control line. Both single-qubit manipulations and two-qubit gates can be realized through parametric modulation. The control scheme gets rid of IQ mixers, dramatically simplifies the input chain and reduces the potential source of errors. The demand for DACs has also been halved, reducing the cost. The rest of this paper is organized as follows. We introduce the control scheme and compare it with conventional methods in Section 2. We explain how to construct universal quantum gates using parametric modulation in Section 3 and analyze the control fidelity

*Project supported by the National Key Research and Development Program of China (Grant No. 2016YFA0301802), the National Natural Science Foundation of China (Grant Nos. 11474152, 12074179, and 61521001), and the Young Fund of Jiangsu Natural Science Foundation of China (Grant No. BK20180750).

†Corresponding author. E-mail: shaoxiong.li@nju.edu.cn
‡Corresponding author. E-mail: tanxs@nju.edu.cn

© 2021 Chinese Physical Society and IOP Publishing Ltd

in Section 4. We summarize the article in the last section.

2. Control scheme

We illustrate our control scheme in Fig. 1(a). A continuous pump signal is injected into the quantum chip through a common drive line, which is coupled to all qubits. The pump signal drives all the qubits non-resonantly. Since the effective drive amplitude on the qubits (tens of megahertz in Rabi frequency) is generally much smaller than the frequency detuning between the qubits and the pump signal, negligible excitation is caused.

To perform gate operations, we parametrically modulate a qubit's frequency with a sinusoidal pulse, through its Z control line. When the frequency of the modulated pulse closely resonates with the detuning between the qubit and the pump signal, single-qubit excitation can be achieved. Two-qubit operations (typically iSWAP-type gates) are realized when the modulation frequency is closely resonant to the detuning between two coupled qubits.

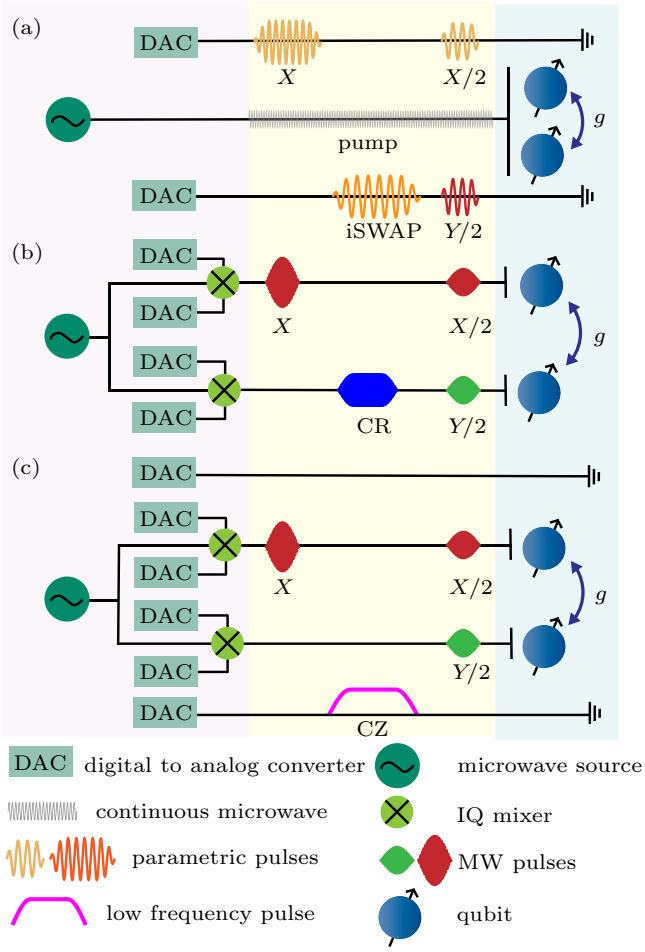


Fig. 1. Illustration of three control schemes: (a) full parametric modulation; (b) full microwave control; (c) hybrid control including microwave control and frequency modulation. The left side shows the electronic circuits of the schemes and the middle part illustrates pulse sequences. The right side represents the quantum devices. For simplicity, control schemes for two coupled qubits are shown.

In the gate scheme, all pulses are directly produced by DACs, without using any IQ mixer for up-conversion. Since the single-qubit gates (SQGs) and iSWAP gates can share the same control line and DACs, an N-qubit chip can be fully controlled by N Z control lines and N DACs. The frequency difference between qubits and the pump signal is about 1 GHz–2 GHz, which means the sampling rate of DACs needs to be about 5 GHz. To reduce the limitations of the scheme, the qubit (typically transmon) can be biased at its sweet spot and the modulation frequency is then halved.[15,16,21,22] Therefore, DACs with a sampling rate of 2 GHz–3 GHz are sufficient for gate operations in experiments (See Supplementary material for details).

Our gate scheme is fully based on the parametric frequency modulation of the qubits. We compare our scheme with conventional control schemes which are based on full microwave modulation[23–26] and the hybrid control.[4,27] In the full microwave scheme, both SQGs and two-qubit gates (typically CR gates) are realized with microwave pulses, which are upconverted from a continuous microwave using IQ mixers. SQGs and two-qubit gates share the same control line and room temperature equipments. In this scheme, two DACs and one mixer are needed to manipulate one qubit, see Fig. 1(b). In the hybrid control scheme, the SQGs are realized by up-converted microwave pulses injected through the XY lines, and two-qubit gates are realized by low-frequency pulses injected through the Z lines, see Fig. 1(c). Although the Z line and XY line can be merged in circuit design,[1,28] the microwave excitation and the frequency modulation still need independent DACs for control. Therefore, in the hybrid scheme, each qubit needs 3 DACs (two for microwave control and one for frequency modulation) and one mixer. The comparison shows that our scheme greatly simplifies the control system and completely gets rid of IQ mixers. Generally, each pump signal can control tens of qubits, with the frequencies of the qubits alternately arranged. For larger-scale quantum computation, more than one pump signals can be introduced.

Although parametric modulation is preferred in our proposal, it is feasible to construct SQGs (iSWAP gates) by tuning qubit frequency into resonance with the pump frequency (frequency of neighboring qubit). However, there are two drawbacks in the latter case: i) The frequency crowding problem: during gate operations, the system may pass through unwanted crossings with neighboring qubit's energy levels, causing state leakage; ii) Generally, the qubits are idly biased at the sweet spot with longer coherent time. Strongly tuning the qubit away from the sweet spot will cause severe decoherence. The parametric modulation enables frequency-selective gates and can effectively avoid these two problems.

3. Universal quantum gates based on parametric modulation

In this section, we theoretically explain how the SQGs and the iSWAP-type gates are constructed in our control scheme. For simplicity, here we consider two coupled qubits Q_1 and Q_2. The coupling strength between the two qubits is g_{12}. The frequency of each qubit is tuned by an external flux signal. A global pump signal of amplitude P is injected into the quantum chip. The system Hamiltonian is (set $\hbar = 1$)

$$\begin{aligned} H =& \sum_{i=1}^{2} \frac{1}{2}(\omega_i + \xi_i(t) + z_i(t))\sigma_i^z \\ &+ \sum_{i=1}^{2} \lambda_i P \cos(\omega_{\rm p} t + \phi_i^{\rm p})\sigma_i^x + g_{12}\sigma_1^x\sigma_2^x, \end{aligned} \tag{1}$$

where λ_i denotes the coupling coefficient between Q_i and the pump signal. Due to different positions on the quantum chip, each qubit senses a different phase $\phi_i^{\rm p}$ caused by the pump signal. Notice that both $\xi_i(t)$ and $z_i(t)$ are frequency bias signals, the former one stands for parametric modulation and the latter one represents trivial Z gate.

Defining $\zeta_i(t) = \int^t \xi_i(\tau)\,{\rm d}\tau$ and the unitary operator

$$U = \exp\left({\rm i} \sum_{i=1}^{2} \frac{\omega_i t + \zeta_i(t) + \phi_i^{\rm p}}{2} \sigma_i^z \right), \tag{2}$$

we get the Hamiltonian in the interaction picture as follows:

$$\begin{aligned} H' =& \sum_{i=1}^{2} \frac{1}{2} z_i(t)\sigma_i^z + \sum_{i=1}^{2} \lambda_i P \frac{\cos(\Delta_{{\rm p}i} t - \zeta_i(t))}{2} \sigma_i^x \\ &+ \sum_{i=1}^{2} \lambda_i P \frac{\sin(\Delta_{{\rm p}i} t - \zeta_i(t))}{2} \sigma_i^y \\ &+ g_{12} \left\{ \exp\left[-{\rm i}(\Delta_{12} t + \zeta_{12}(t) + \phi_{12}^{\rm p}) \right] \sigma_1^+ \sigma_2^- \right. \\ &\left. + \exp\left[{\rm i}(\Delta_{12} t + \zeta_{12}(t) + \phi_{12}^{\rm p}) \right] \sigma_1^- \sigma_2^+ \right\}. \end{aligned} \tag{3}$$

Here $\Delta_{12} = \omega_1 - \omega_2$, $\Delta_{{\rm p}i} = \omega_{\rm p} - \omega_i$, $\zeta_{12}(t) = \zeta_1(t) - \zeta_2(t)$, and $\phi_{12}^{\rm p} = \phi_1^{\rm p} - \phi_2^{\rm p}$. We have made a rotating wave approximation (RWA) by omitting counter-rotating-wave terms ($e^{{\rm i}(\omega_i + \omega_{\rm p})}$). Equation (3) provides a possibility to realize universal quantum gates. The terms in the first line are corresponding to single-qubit rotations and the terms in the second line are related to iSWAP-type gates.

3.1. Single-qubit gates

For SQGs, we consider the single qubit Q_1. The corresponding modulation signal is in derivative form $\xi_1(t) = \zeta_1'(t)$, where $\zeta_1(t) = A(t)\sin(\Delta_{\rm p1} t + \phi^{\rm f})$. Using Jacobi–Anger expansion, the first three terms in Eq. (3) becomes

$$\begin{aligned} H'_{\rm SQG} =& \frac{1}{2} z_1(t)\sigma_1^z + \lambda_1 P \frac{{\rm J}_1(A(t))\cos(\phi^{\rm f})}{2} \sigma_1^x \\ &- \lambda_1 P \frac{{\rm J}_1(A(t))\sin(\phi^{\rm f})}{2} \sigma_1^y, \end{aligned} \tag{4}$$

where ${\rm J}_n(z)$ is the n-th-order Bessel function of the first kind. The rapid oscillation terms in the expansion are omitted using RWA, the effect of these terms will be discussed in Section 4. The phase $\phi^{\rm f}$ controls the direction of XY rotation and

$$\theta_1 = \int_0^{t_{\rm g}} \lambda_1 P {\rm J}_1(A(t))\,{\rm d}t \tag{5}$$

is the rotation angle. Here, $t_{\rm g}$ represents the gate time. The rotation angle of Z gate is $\int_0^{t_{\rm g}} z_1(t)\,{\rm d}t$. In real experiments, the Z gates can also be constructed by updating phases of subsequent rotations, known as virtual Z gates.[29,30]

3.2. iSWAP-type gates

For two-qubit gates between two coupled qubits Q_1 and Q_2, we consider a sinusoidal signal $\zeta_1(t) = A(t)\sin(-\Delta_{12} t + \phi^{\rm f})$ on Q_1 (and $\zeta_2(t) = 0$ on Q_2). The effective interaction Hamiltonian between Q_1 and Q_2 is

$$\begin{aligned} H'_{\rm I} =& g_{12}{\rm J}_1(A(t)) \left\{ \exp\left[-{\rm i}(\phi_{12}^{\rm p} + \phi^{\rm f}) \right] \sigma_1^+ \sigma_2^- \right. \\ &\left. + \exp\left[{\rm i}(\phi_{12}^{\rm p} + \phi^{\rm f}) \right] \sigma_1^- \sigma_2^+ \right\}, \end{aligned} \tag{6}$$

with fast oscillation terms omitted by RWA. The corresponding unitary operator of the iSWAP-type gate is

$$\hat{U} = \begin{bmatrix} 1 & 0 & 0 & 0 \\ 0 & \cos(\theta/2) & -{\rm i}e^{-{\rm i}\phi}\sin(\theta/2) & 0 \\ 0 & -{\rm i}e^{{\rm i}\phi}\sin(\theta/2) & \cos(\theta/2) & 0 \\ 0 & 0 & 0 & 1 \end{bmatrix}, \tag{7}$$

where $\theta = 2\int_0^{t_{\rm g}} g_{12}{\rm J}_1(A(t))\,{\rm d}t$ represents rotation angle in the subspace of $\{01, 10\}$, and $\phi = \phi_{12}^{\rm p} + \phi^{\rm f}$ determines the rotation direction. The iSWAP ($\sqrt{\rm iSWAP}$) gate is constructed by setting $\theta = \pi$ ($\theta = \pi/2$) and $\phi = 0$.

3.3. Phase accumulation

For SQGs, the phases of pump signal $\phi_i^{\rm p}$ sensed by the qubits are absorbed in the unitary operator (Eq. (2)). The direction of XY rotation is controlled by the phase of the modulation signal $\phi^{\rm f}$. For iSWAP-type gates, there is an additional phase difference $\phi_{12}^{\rm p} = \phi_1^{\rm p} - \phi_2^{\rm p}$. This phase difference, together with the phase latency between control chains, is compensated by adjusting $\phi^{\rm f}$.

In real experiments, the non-resonance terms in the Jacobi–Anger expansion will cause frequency shift of the qubits during parametric modulation, known as Stark shift.[31,32] The frequency shift will introduce an additional phase accumulation on the qubits. The phase accumulations become more complicated when considering higher energy levels and nonlinear frequency response to external signal

(Ref. [15] and Supplementary material). The phase accumulations can be measured by Ramsey experiments and cancelled by virtual Z gates.[29]

It is worth mentioning that the actual frequency modulation $\xi(t)$ is the derivation of primitive function: $\xi(t) = \zeta'(t) = A'(t)\sin(\omega t + \phi^{\rm f}) + \omega A(t)\cos(\omega t + \phi^{\rm f})$. $\xi(t)$ is also a sinusoidal modulation, the phase of $\xi(t)$ is

$$\phi_{\rm m}(t) = \phi^{\rm f} - \arctan\left(\frac{A'(t)}{\omega A(t)}\right). \tag{8}$$

If the envelope $A(t)$ is slowly varied compared to ω ($A'(t) \ll \omega A(t)$), the phase can be approximated by $\phi_{\rm m} = \phi^{\rm f}$.

4. Error analysis

In the above discussion, only the resonant term ($n = 1$) in the Jacobi–Anger expansion is considered. While the non-resonant interaction terms ($n \neq 1$) may cause unwanted transition and damage the control fidelity. We can use a simplified Rabi model to estimate the transition errors. During the parametric control, both the interaction strength Ω and the detuning Δ of a non-resonant interaction in the Rabi model are treated as constants. The transition rate caused by the non-resonant interaction is

$$\varepsilon = \frac{1}{2}\frac{\Omega^2}{\Omega^2 + \Delta^2}\left[1 - \cos(\sqrt{\Omega^2 + \Delta^2}t)\right]. \tag{9}$$

In the case of large detuning ($\Delta \gg \Omega \sim 1/T_{\rm gate}$), ε is a rapid oscillation term. We use the average value to evaluate the gate error, the transition rate can be simplified as $\varepsilon \simeq \Omega^2/2\Delta^2$. Since typical superconducting qubits such as transmons and C-shunted flux qubits are weakly anharmonic,[33,34] the error analysis should include the second excitation level. Thus, the lowest three levels of each qubit are considered in the following discussion.

4.1. Errors of the parametric SQGs

With the sinusoidal modulation $\zeta(t) = A(t)\sin(\omega t + \phi^{\rm f})$, the Hamiltonian for the parametric SQGs is

$$\begin{aligned} H_{\rm SQG} = &\sum_{n=-\infty}^{\infty} \frac{B}{2} {\rm J}_n(A(t)) {\rm e}^{{\rm i}(-n\omega t - n\phi^{\rm f} + \Delta_{\rm p1} t)} |1\rangle\langle 0| \\ &+ \sum_{n=-\infty}^{\infty} \frac{\sqrt{2}B}{2} {\rm J}_n(A(t)) {\rm e}^{{\rm i}(-n\omega t - n\phi + \Delta_{\rm p1} t - \alpha_1 t)} |2\rangle\langle 1| + {\rm h.c.}, \end{aligned} \tag{10}$$

where α_1 is the anharmonicity of the qubit Q_1 and $\Delta_{\rm p1}$ is the detuning between pump signal and Q_1. $B = \lambda P$ denotes the effective pump strength on the qubit.

The parametric SQGs are realized by setting the first order Bessel interaction into resonance ($\omega = \Delta_{\rm p1}, n = 1$). All the other terms are non-resonant interactions, the corresponding interaction strength and the estimated error rates with typical parameters are shown in Table 1. According to Eq. (9), the terms with relatively small detuning and large interaction strength generally cause dominant errors. Assuming the modulation amplitude is smaller than the detuning ($|A(t)| < 1$), the terms with $n > 1$ and $n < 0$ can be neglected since these terms have both small interaction strength and large detuning. Notice that the transition errors should be multiplied by an extra factor f. For example, the error rates caused by interactions in subspace $\{|1\rangle, |2\rangle\}$ should be multiplied by $f = 0.5$, since such an interaction has no effect if the qubit is in state $|0\rangle$.

All transition errors scale quadratically with the pump strength B, as shown in Fig. 2(a). Since ${\rm J}_0(A(t)) \sim 1$ with $A(t) < 1$, the 0th-order error is almost independent of the modulation amplitude $A(t)$. But the 1st-order interaction in $\{|1\rangle, |2\rangle\}$ subspace is strongly related to the modulation amplitude. This error becomes dominant with large $A(t)$, shown as the dashed blue line in Fig. 2(a). There is a trade-off between the gate time and the transition errors. Stronger pump strength B or modulation strength $A(t)$ will result in shorter gate time but cause more transition errors. In all, we find that total error rates are smaller than 0.1%, with a gate time of about 60 ns.

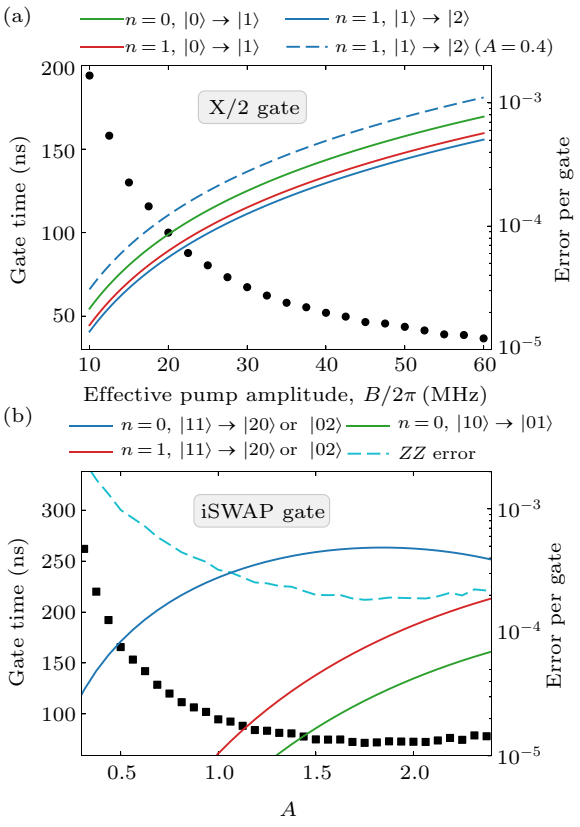


Fig. 2. Error analysis of parametric modulation. (a) Gate time (black circles) and transition errors (solid lines) of $X/2$ gate *versus* pump strength B, with modulation factor $A = 0.27$. The detuning between qubit's frequency and the pump frequency is $\Delta_{\rm p1}/2\pi = 1.5$ GHz. The anharmonicity of the qubit is $\alpha_1/2\pi = -250$ MHz. State leakage arising from 1st-order Bessel interaction becomes dominant in case of strong modulation amplitude ($A = 0.4$), shown as the dashed blue line. (b) Gate time (black squares) and transition errors (solid lines) of iSWAP gates versus modulation factor A. The detuning between the two qubits is $\Delta_{12}/2\pi = 800$ MHz and the coupling strength strength is $g_{12}/2\pi = 6.7$ MHz. The anharmonicities of both qubits are set as -250 MHz. The dashed black line shows the ZZ interaction error during the parametric modulation.

Table 1. Non-resonant interactions in a parametric SQG. The error rates are evaluated as $(\Omega^2/2\Delta^2)f$, with $B/2\pi = 30$ MHz, $\Delta_{p1}/2\pi = 1.5$ GHz, $\alpha_1/2\pi = -250$ MHz, and $A(t) = 0.27$.

Subspace	Bessel order	Ω	Δ	f	Error rate
$\|0\rangle$,$\|1\rangle$	$n = 0$	$BJ_0(A(t))/2$	Δ_{p1}	1	1.9×10^{-4}
	$n \neq 0,1$	$BJ_n(A(t))/2$	$(1-n)\Delta_{p1}$	1	$< 1 \times 10^{-6}$
$\|1\rangle$,$\|2\rangle$	$n = 0$	$\sqrt{2}BJ_0(A(t))/2$	$\Delta_{p1} + \alpha_1$	0.5	1.4×10^{-4}
	$n = 1$	$\sqrt{2}BJ_1(A(t))/2$	α_1	0.5	1.2×10^{-4}
	$n \neq 0,1$	$\sqrt{2}BJ_n(A(t))/2$	$(1-n)\Delta_{p1} + \alpha_1$	0.5	$< 1 \times 10^{-6}$

4.2. Errors of the iSWAP gate

Similar error analysis can be given to the iSWAP gates. The interaction Hamiltonian for two-qubit gates between Q_1 and Q_2 is

$$\begin{aligned} H_{\rm I} = \sum_{n=-\infty}^{\infty} & g_{12} e^{i(\Delta_{12}t+\phi_{12}^{p})} \{ J_n(A(t)) e^{i(n\omega t+n\phi)} |01\rangle\langle 10| \\ & + \sqrt{2} J_n(A(t)) e^{i(n\omega t+\alpha_1 t+n\phi)} |11\rangle\langle 20| \\ & + \sqrt{2} J_n(A(t)) e^{i(n\omega t-\alpha_2 t+n\phi)} |02\rangle\langle 11| \} + \text{h.c.} \end{aligned} \quad (11)$$

The resonant condition is $\Delta_{12} + \omega = 0$. We show the non-resonant interaction terms in Table 2. Error rates caused by the terms with $n > 1$ or $n < 0$ are negligible. Notice that the strength of 0th-order interaction is in form of $1 - J_0(A)$, instead of $J_0(A)$, in the dressed eigenstates basis. The corresponding error rates of iSWAP gates *versus* modulation amplitude are shown in Fig. 2(b). The 1st-order terms in the subspace of $\{|11\rangle, |20\rangle\}$ and $\{|11\rangle, |02\rangle\}$ are the dominant sources of errors.

In addition to transition errors, there is also intrinsic ZZ error. The ZZ coupling strength is defined as $\eta = \omega_{11} + \omega_{00} - \omega_{01} - \omega_{10}$.[35–37] Due to the level repulsion effect of higher levels, the ZZ coupling strength between two coupled qubits is[38,39]

$$\eta = 2g_{12}^2 \frac{\alpha_1 + \alpha_2}{(\Delta_{12} - \alpha_1)(\Delta_{12} + \alpha_2)}. \quad (12)$$

During the iSWAP gates, there is a conditional phase accumulation on state $|11\rangle$, denoted as $\Delta\phi_{zz} = \int \eta \, dt$ on state $|11\rangle$. The ZZ error is evaluated as $\varepsilon_{zz} = \Delta\phi_{zz}^2/4$, which is an upper limit estimate. The ZZ phase error increases with gate time, shown as the dashed black line in Fig. 2(b). One may try to shorten the gate time by making the coupling strength g_{12} stronger. However this will also cause more ZZ phase error, since the ZZ interaction strength quadratically depends on the coupling strength.

Table 2. Non-resonant interactions in a parametric iSWAP gate. The error rates are calculated with $g_{12}/2\pi = 6.7$ MHz, $\Delta_{12}/2\pi = 800$ MHz, $\alpha_1/2\pi = \alpha_2/2\pi = -250$ MHz, and $A(t) = 1$.

Subspace	Bessel order	Ω	Δ	f	Error rate
$\|01\rangle$,$\|10\rangle$	$n = 0$	$2g_{12}(1 - J_0(A(t)))$	Δ_{12}	0.5	3.8×10^{-6}
	$n \neq 0,1$	$2g_{12}J_n(A(t))$	$(1-n)\Delta_{12}$	0.5	$< 1 \times 10^{-6}$
$\|11\rangle$,$\|20\rangle$	$n = 0$	$2\sqrt{2}g_{12}(1 - J_0(A(t)))$	$\Delta_{12} + \alpha_1$	0.25	8.2×10^{-6}
	$n = 1$	$2\sqrt{2}g_{12}J_1(A(t))$	α_1	0.25	1.4×10^{-4}
	$n \neq 0,1$	$2\sqrt{2}g_{12}J_n(A(t))$	$(1-n)\Delta_{12} + \alpha_1$	0.25	1×10^{-6}
$\|02\rangle$,$\|11\rangle$	$n = 0$	$2\sqrt{2}g_{12}(1 - J_0(A(t)))$	$\Delta_{12} - \alpha_2$	0.25	2.2×10^{-6}
	$n = 1$	$2\sqrt{2}g_{12}J_1(A(t))$	$-\alpha_2$	0.25	1.4×10^{-4}
	$n \neq 0,1$	$2\sqrt{2}g_{12}J_n(A(t))$	$(1-n)\Delta_{12} - \alpha_2$	0.25	$< 1 \times 10^{-6}$

5. Summary

We propose a universal control scheme based on parametric frequency modulation. By halving the required DAC, this control scheme effectively saves the cost of large-scale quantum control. The input system has been greatly simplified. Because no IQ mixer is used, complicated calibration work is avoided. We theoretically explain how the universal gates are constructed by introducing a global microwave pump. The fidelity analysis shows that The error rate of parametric control is below 0.1% with a typical gate time of 60 ns (100 ns) for single-qubit (two-qubit) gates, proving its potential for a broad application.

References

[1] Arute F, Arya K, Babbush R, Bacon D, *et al.* 2019 *Nature* **574** 505
[2] You J and Nori F 2011 *Nature* **474** 589
[3] Jurcevic P, Javadi-Abhari A, Bishop L S, *et al.* 2020 arXiv preprint arXiv: 2008.08571
[4] Song C, Xu K, Liu W, *et al.* 2017 *Phys. Rev. Lett.* **119** 180511
[5] Liu W Y, Zheng D N and Zhao S P 2018 *Chin. Phys. B* **27** 027401
[6] Preskill J 2018 *Quantum* **2** 79
[7] Li M, Tan X, Dai K, Zhao P, Yu H and Yu Y 2018 *Chin. Phys. B* **27** 063202

[8] Gong M, Wang S, Zha C, *et al.* 2021 arXiv preprint arXiv: 2102.02573
[9] Xu H, Liu W, Li Z, *et al.* 2021 *Chin. Phys. B* **30** 044212
[10] Raftery J, Vrajitoarea A, Zhang G, Leng Z, Srinivasan S and Houck A 2017 arXiv preprint arXiv: 1703.00942
[11] Li Z Y, Yu H F, Tan X S, Zhao S P and Yu Y 2019 *Chin. Phys. B* **28** 098505
[12] Jolin S, Borgani R, Tholén M, Forchheimer D and Haviland D 2020 arXiv preprint arXiv: 2008.07265
[13] Kalfus W D, Lee D F, Ribeill G J, Fallek S D, Wagner A, Donovan B, Ristè D and Ohki T A 2020 arXiv preprint arXiv: 2008.02873
[14] Xu Y, Huang G, Santiago D I and Siddiqi I 2020 arXiv preprint arXiv: 2101.00066
[15] Caldwell S, Didier N, Ryan C, *et al.* 2018 *Phys. Rev. Appl.* **10** 034050
[16] Didier N, Sete E A, da Silva M P and Rigetti C 2018 *Phys. Rev. A* **97** 022330
[17] Silveri M, Tuorila J, Thuneberg E and Paraoanu G 2017 *Rep. Prog. Phys.* **80** 056002
[18] Reagor M, Osborn C B, Tezak N, *et al.* 2018 *Sci. Adv.* **4** eaao3603
[19] Li X, Ma Y, Han J, Chen T, *et al.* 2018 *Phys. Rev. Appl.* **10** 054009
[20] Chu J, Li D, Yang X, *et al.* 2020 *Phys. Rev. Appl.* **13** 064012
[21] Koch J, Terri M Y, Gambetta J, Houck A A, Schuster D, Majer J, Blais A, Devoret M H, Girvin S M and Schoelkopf R J 2007 *Phys. Rev. A* **76** 042319
[22] McKay D C, Filipp S, Mezzacapo A, Magesan E, Chow J M and Gambetta J M 2016 *Phys. Rev. Appl.* **6** 064007
[23] Chow J M, Córcoles A, Gambetta J M, *et al.* 2011 *Phys. Rev. Lett.* **107** 080502
[24] Rigetti C and Devoret M 2010 *Phys. Rev. B* **81** 134507
[25] Sheldon S, Magesan E, Chow J M and Gambetta J M 2016 *Phys. Rev. A* **93** 060302
[26] Krinner S, Kurpiers P, Royer B, Magnard P, Tsitsilin I, Besse J C, Remm A, Blais A and Wallraff A 2020 *Phys. Rev. Appl.* **14** 044039
[27] Barends R, Kelly J, Megrant A, *et al.* 2014 *Nature* **508** 500
[28] Xu Y, Chu J, Yuan J, *et al.* 2020 arXiv preprint arXiv: 2006.11860
[29] McKay D C, Wood C J, Sheldon S, Chow J M and Gambetta J M 2017 *Phys. Rev. A* **96** 022330
[30] Johnson B R, da Silva M P, Ryan C A, Kimmel S, Chow J M and Ohki T A 2015 *New J. Phys.* **17** 113019
[31] Schuster D, Wallraff A, Blais A, Frunzio L, Huang R S, Majer J, Girvin S M and Schoelkopf R J 2005 *Phys. Rev. Lett.* **94** 123602
[32] Motzoi F, Gambetta J M, Rebentrost P and Wilhelm F K 2009 *Phys. Rev. Lett.* **103** 110501
[33] Yan F, Gustavsson S, Kamal A, *et al.* 2016 *Nat. Commun.* **7** 12964
[34] You J, Hu X, Ashhab S and Nori F 2007 *Phys. Rev. B* **75** 140515
[35] Xu X and Ansari M 2020 arXiv preprint arXiv: 2009.00485
[36] Xu H, Song C, Liu W, *et al.* 2016 *Nat. Commun.* **7** 11018
[37] Sung Y, Ding L, Braumüller J, *et al.* 2020 arXiv preprint arXiv: 2011.01261
[38] Zhao P, Xu P, Lan D, Chu J, Tan X, Yu H and Yu Y 2020 *Phys. Rev. Lett.* **125** 200503
[39] Zhao P, Lan D, Xu P, Xue G, Blank M, Tan X, Yu H and Yu Y 2020 arXiv preprint arXiv: 2011.03976